The structure of diphosphaallenic radical cations as evidenced by EPR experiments and *ab initio* calculations

Mostafa Chentit,[a] Helena Sidorenkova,[a] Abdelaziz Jouaiti,[a] Gustavo Terron,[a] Michel Geoffroy *,[a] and Yves Ellinger *,[b]

[a] *Department of Physical Chemistry, University of Geneva, 30 Quai E. Ansermet,*
1211 Geneva 4, Switzerland
[b] *Laboratoire de Radioastronomie, Ecole Normale Supérieure, 24 rue Lhomond, 75005 Paris,*
France

The isotropic hyperfine coupling constants of the diphosphaalkene radical cation have been measured by EPR spectroscopy after electrochemical oxidation of ArP=C=PAr (and ArP=^{13}C=PAr) in tetrahydrofuran (THF). The two ^{31}P constants as well as the ^{13}C coupling are close to 90 MHz. Taking HPCPH as a model compound, the structure has been assessed, by extensive *ab initio* calculations including correlation effects at the MP2 and MCSCF levels of theory. It is found that oxidation of the allenic −P=C=P− structure leads to the formation of two rotamers with HPPH dihedral angles of 45° and 135°. These two structures are compatible with the Jahn–Teller distortion of allene. The calculated hyperfine constants support the EPR results.

Introduction

With their two adjacent perpendicular π systems, allene derivatives are fascinating species for both experimentalists and theoreticians. Numerous studies have been devoted to these molecules[1,2] and to their singly and doubly charged positive ions.[3–8] In recent years, special attention has been given to cumulenes containing one or two atoms of group VB[9,10] (*e.g.* RP=C=PR). This interest is mainly due to the considerable progress made in synthetic chemistry, especially in the field of phosphorus-containing compounds in low coordination states,[11] and to a better understanding of the redox properties of these compounds.[12] Crystal structures of diphosphaallenes stabilized by bulky substituents **1** have shown that the P−C−P sequence is not linear and that these molecules adopt a structure close to C_2 symmetry, with the substituents on the opposite sides of the PCP plane.[13] The structure of the first term of the series, HPCPH **2**, has been the subject of several *ab initio* studies,[9,14] all of which reproduce the characteristics of the X-ray measurements.

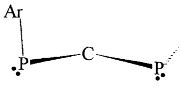

Ar = 2,4,6-(Bu^t)$_3$C$_6$H$_2$

1

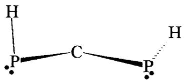

2

The geometry of these allenic systems is expected to be quite sensitive to oxidation. Taking H$_2$C=C=CH$_2$, **3**, as an example, removal of one electron creates an open shell system with three electrons distributed in a set of degenerate π orbitals; this situation results in a Jahn–Teller distortion which causes the molecular frame to relax from D_{2d} symmetry in the neutral system to D_2 in the positive ion **4** with the dihedral angle between the two CH$_2$ planes passing from 90° to 40°.[3,15]

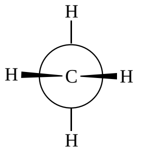

3

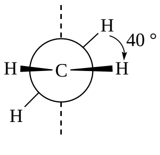

4

The modifications of the geometry following oxidation are much less clear when hetero-atoms are part of the allenic system; nitrilimine (HCNNH), for example, adopts a nonplanar allenic structure but the corresponding cation has been predicted to have a planar propynylic structure.[16] In the present study, our purpose is two-fold: (*i*) to generate the radical cation $\mathbf{1}^{\cdot +}$ and obtain information on its structure from its hyperfine coupling constants, (*ii*) link these results to an accurate *ab initio* description of the model system **2** and its structural changes when the radical cation $\mathbf{2}^{\cdot +}$ is formed.

Experimental

Synthesis

1,3-Diphosphaallene[13,17] was synthesized following the methods of Yoshifuji[18] and of Krieger.[19] The ^{13}C enriched compound ArP=^{13}C=PAr was synthesized using the latter method: ArPH$_2$ (0.5 g, 1.8 mmol) was first reacted with BuLi (1.8 mmol) in dried diethyl ether at room temp.; after successive additions, at room temp., of Me$_3$SiCl (1.8 mmol) and BuLi (1.8 mmol) the reaction mixture was cooled to 0 °C and ^{13}CS$_2$ (0.9 mmol) was added dropwise to the solution. After 1 h, the mixture was slowly warmed to room temp. ArP=^{13}C=PAr was purified on a column using pentane as an eluent (mp 202–204 °C; δ_P 141).

Generation of the radical cation and EPR experiments

EPR measurements were carried out on a Bruker-200 D spectrometer (X-band, 100 kHz magnetic field modulation) equipped with a variable temperature attachment. Radical cation $\mathbf{1}^{\cdot +}$ was generated by electrochemical oxidation of a solution of **1** (10^{-2} M) in THF in presence of Bu$_4$NPF$_6$. This electrolysis was performed *in situ* in the EPR cavity using platinum wires as electrodes and a PAR potentiostat.

Calculations

All calculations were carried out with GAUSSIAN92[20] and HONDO8.5.[21] The orbital densities and vibrational analysis have been performed with the MOLEKEL molecular graphics package.[22]

Results and discussion

EPR spectra

An example of an EPR spectrum obtained at 300 K with an

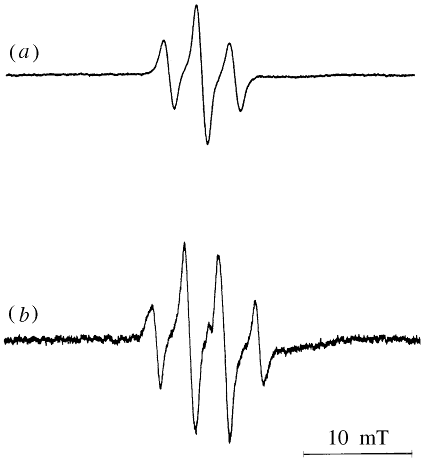

Fig. 1 EPR spectrum obtained after electrochemical reduction of a solution of: (*a*) ArP=C=PAr in THF; (*b*) ArP=^{13}C=PAr in THF

electrolysed solution of **1** using a potential of +1.5 V is shown in Fig. 1(*a*). While the solution remained liquid, this spectrum was not very sensitive to a decrease in temperature; when the solution was frozen, however, the signal disappeared, probably due to a considerable broadening of the lines. A subsequent reheating led to the reappearance of the spectrum, even in the absence of a new electrolysis. At room temperature, the spectrum persisted for *ca.* 20 min after the electrolysis had been stopped. There is no doubt that the two coupling constants of 87 MHz observed in the EPR spectrum obtained with ArP=C=PAr [Fig. 1(*a*)] are caused by hyperfine couplings with two equivalent ^{31}P nuclei. As shown in Fig. 1(*b*), isotopic ^{13}C substitution of the central carbon leads to a new spectrum which is characterized by an additional coupling constant close to 87 MHz.

The absence of any proton hyperfine splitting in the spectrum shown in Fig. 1 suggests that, as for **1**, the plane of each aromatic ring remains perpendicular to the corresponding $C_{(Ar)}PC$ plane in the radical cation. Moreover, comparison of the ^{31}P and ^{13}C couplings with the corresponding atomic constants[23] indicates that the participation of the phosphorus and carbon s orbitals to the unpaired spin distribution are very small, *i.e.* $\rho_{s(C)} = 87/3777 = 0.023$; $\rho_{s(P)} = 87/13306 = 0.006$.

In a very rough approximation, we can assume that the observed Fermi contact interaction is only due to inner shell polarization. In this hypothesis, the p spin densities can be estimated from previous single crystal studies on the triptycyl–PH[24] and $(COO^-)_2\,^{13}CH$;[25] this leads to a spin density of 0.21 in a p orbital of each phosphorus and of 0.51 in a p orbital of the carbon atom. This description is not in conflict with that proposed for $[R_2C{=}C{=}CR_2]^{\bullet +}$ by Bolze *et al.*[26] which states that the unpaired electron is equally distributed in a p orbital on each terminal atom and two p orbitals of the central carbon. However, this description relies on crude approximations to the spin distribution which neglects, *inter alia*, all nearest neighbour interactions (*i.e.* spin polarization through σ_{PC} bonds); quantum chemistry calculations, indispensable to a better understanding of the spin properties, are reported in the following section.

Quantum chemical calculations

The calculation of each species as $(2,4,6\text{-}Bu^t_3C_6H_2){-}P{=}C{=}P{-}(2,4,6\text{-}Bu^t_3C_6H_2)$ is far beyond the present capabilities of quantitative *ab initio* methods. The simplest system that retains the characteristics of 1,3-diphosphaallenes derivatives is HP=C=PH where H atoms replace the bulky groups without loss of generality in the allenic linkage. In terms of Lewis localized orbitals of the σ backbone, the electronic configuration of the neutral system is given by formula (1), where the four

$$[\text{core}]^{12}\ \sigma_{PH}{}^2\sigma_{PH}{}^2\sigma_{PC}{}^2\sigma_{PC}{}^2 lp_1{}^2 lp_2{}^2\pi_1{}^2\pi_2{}^2 \qquad (1)$$

highest orbitals, namely, the two lone pairs on phosphorus atoms and the two π bonds, contain the eight most active electrons of this system, one of which is removed by the oxidation process.

Neutral HPCPH. This system has already been the subject of a few theoretical investigations that predicted an allenic type structure.[9,14] As a preliminary study aimed at understanding how this system is affected by oxidation we reconsidered its structure at several levels of theory. Standard 6-31G* and 6-311G** basis sets were employed and correlation effects were first included at the MP2 level with no frozen electrons. Anticipating the need for a multiconfigurational treatment of the open-shell cation in view of the shape of the highest orbitals, CASSCF calculations, hereafter referred to as (CAS/basis set), were also carried out. The complete active space is generated by distributing eight electrons, all possible ways, in the two lone pairs on the phosphorus atoms and in the four π bonding and antibonding orbitals [formula (2)]. The core contains the inner

$$[\text{core}]^{20}\ [lp_1 lp_2 \pi_1 \pi_2 \pi_1{}^* \pi_2{}^*]^8 \qquad (2)$$

shells and the σ_{PH} and σ_{PC} bonds. A second MCSCF calculation (hereafter referred to as MC/basis set) was carried out in the full valence space with 16 electrons in 14 orbitals in order to account for correlation effects on the σ bond distances, *i.e.*, formula (3). In this treatment, the core consists of the inner

$$[\text{core}]^{12}$$
$$[\sigma_{PH}\sigma_{PH}\sigma_{PC}\sigma_{PC} lp_1 lp_2 \pi_1 \pi_2 \pi_1{}^* \pi_2{}^* \sigma_{PH}{}^* \sigma_{PH}{}^* \sigma_{PC}{}^* \sigma_{PC}{}^*]^{16} \qquad (3)$$

shells of the carbon and phosphorus atoms and all antibonding orbitals are used in the definition of the active space; the internal level of excitation is limited to doubly excited states with respect to the reference determinant, a level which ensures a correct description of electronic correlation for structural studies. The optimized structures are reported in Table 1.

The important point to be noted is that the molecule adopts a C_2 allenic structure with the PH bonds belonging in perpendicular planes, at all levels of theory. The PCP backbone is not linear, because the phosphorus atoms each bear one lone pair and one PH bond; this difference with the terminal carbons of allene that are symmetrically linked to two hydrogens is at the origin of the torsion. On the other hand, the PCP bond angle presents small variations according to the level of electron correlation, the values calculated in the limited CASSCF treatment (*2*) being systematically smaller than those obtained when all bonding electrons are correlated [MP2 or MCSCF (3)]. For the P–H and P–C bonds, the correlated treatments give very similar bond lengths. If we now look at HPCPH to assess the validity of the model for representing the larger systems, it is clear that the geometrical parameters deduced from X-ray experiments (PC = 1.635 Å; ∠PCP = 172.6°; ∠CPC = 100.3°) are well reproduced; the deviation of *ca.* 5° in the bond angles is not surprising in view of the considerable steric repulsion of the aryl groups.

Radical cation of HPCPH. The same series of calculations was performed on the positive ion, including correlation effects at the MP2 and MCSCF levels of theory. The CASSCF treatment corresponds now to an active space generated by distributing seven electrons in six orbitals *i.e.* formula (4). Here the

$$[\text{core}]^{20}\ [lp_1 lp_2 \pi_1 \pi_2 \pi_1{}^* \pi_2{}^*]^7 \qquad (4)$$

core contains the inner shells and the σ_{PH} and σ_{PC} bonds. In order to check for a possible influence of the PCP σ backbone, the single and double MCSCF calculation designed for the neutral system (MC/6-311G**), was carried out in the

Table 1 Optimized parameters and energies for neutral HPCPH **2**

Level	Parameters						Energies/au
	r(P–C)/Å	r(P–H)/Å	∠PCP (°)	∠HΠX (°)	Dihedral angle HPCP (°)	Dihedral angle HPPH (°)	
MP2/6-31G**	1.656	1.414	171.1	95.3	135.3	90.1	−720.7681
MP2/6-311G**	1.653	1.418	170.3	94.9	135.3	90.1	−721.0775
CAS/6-31G**	1.659	1.411	167.6	97.6	135.4	90.6	−720.4509
CAS/6-311G**	1.657	1.413	167.5	97.7	135.0	91.4	−720.5018
MC/6-31G**	1.659	1.434	171.9	97.2	135.3	90.2	−720.5352
MC/6-311G**	1.657	1.436	171.2	97.3	135.3	90.4	−720.8693

Table 2 Optimized parameters and energies for HPCPH cation $\mathbf{2}^{\bullet +}$ (1 cal = 4 184 J)

Level	Parameters						Energies/au	ΔE/kcal mol^{-1}
	r(P–C)/ Å	r(P–H)/ Å	∠PCP (°)	∠HPC (°)	Dihedral angle HPCP (°)	Dihedral angle HPPH (°)		
cis-like								
MP2/6-31G**	1.640	1.414	162.7	95.6	−157.2	46.8	−720.4328	0.0
MP2/6-311G**	1.640	1.419	162.7	94.7	−157.2	46.7	−720.7389	0.0
CAS/6-31G**	1.666	1.404	156.6	98.6	−158.6	45.8	−720.1470	0.0
CAS/6-311G**	1.662	1.408	158.6	97.8	−158.6	44.8	−720.1965	0.0
MC/6-31G**	1.672	1.428	163.3	96.0	−157.3	46.5	−720.2330	0.0
MC/6-311G**	1.668	1.433	157.3	95.6	−157.1	47.0	−720.2838	0.0
trans-like								
MP2/6-31G**	1.638	1.415	179.1	96.2	−113.7	132.7	−720.4318	0.63
MP2/6-311G**	1.638	1.420	179.1	95.1	−113.7	132.6	−720.7376	0.82
CAS/6-31G**	1.654	1.403	176.4	100.1	−113.2	133.4	−720.1439	1.95
CAS/6-311G**	1.652	1.407	175.7	99.8	−113.6	133.5	−720.1932	2.07
MC/6-31G**	1.669	1.428	178.7	96.2	−113.4	133.4	−720.2324	0.38
MC/6-311G**	1.665	1.433	178.9	95.7	−113.6	132.9	−720.2830	0.50

Table 3 Vibrational analysis of minimum energy structures of HPCPH and of its radical cation $\mathrm{HPCPH}^{\bullet +}$: frequencies, ν/cm^{-1}, and (in parentheses), intensities, i/km mol $^{-1}$

Vibration	Neutral MP2/6-311G**	Cation *cis*-like MP2/6-311G**	Cation *trans*-like MP2/6-311G**
asym PH str	2293(73)	2298(52)	2292(54)
sym PH str	2292(51)	2297(3)	2293(2)
asym PC str	1313(13)	1238(1656)	1249(1555)
asym HPC bend	818(79)	630(103)	745(129)
sym HPC bend	810(32)	870(113)	769(6)
HPPH tors	642(0)	693(0)	673(0)
sym PC str	545(0)	596(0)	574(0)
// PCP bend	246(8)	247(6)	245(15)
⊥ PCP bend	244(12)	261(24)	228(6)
ZPE (au)	0.020 96	0.020 80	0.020 66

full valence space of the cation with 15 electrons in 14 orbitals [formula (5)]. Limiting the internal level of excitation to

$$[\mathrm{core}]^{12}$$

$$[\sigma_{\mathbf{PH}}\sigma_{\mathbf{PH}}\sigma_{\mathbf{PC}}\sigma_{\mathbf{PC}}\mathrm{lp}_{\mathbf{1}}\mathrm{lp}_{\mathbf{2}}\pi_{\mathbf{1}}\pi_{\mathbf{2}}\pi_{\mathbf{1}}{}^{*}\pi_{\mathbf{2}}{}^{*}\sigma_{\mathbf{PH}}{}^{*}\sigma_{\mathbf{PH}}{}^{*}\sigma_{\mathbf{PC}}{}^{*}\sigma_{\mathbf{PC}}{}^{*}]^{\mathbf{15}} \qquad (5)$$

diexcited states with respect to the reference determinant has already proved successful in calculations on free radicals delocalized on three centres.[27] The results of the geometry optimization are presented in Table 2. All these correlated treatments show two different minima with C_2 symmetry, hereafter referred to as the *cis*-like (**5**) and *trans*-like (**6**) structures, with a small energy difference in favour of the former [between 0.4 and 0.8 kcal mol^{-1} (1 cal = 4.184 J) when the σ bonds are correlated]. Inclusion of zero-point energies (Table 3) does not modify the present conclusion.

The first point to emerge from the calculations is that the minimum energy structures differ from the neutral parent by an opposite rotation of the P–H bonds. The *cis*-like structure is obtained by rotating these bonds so as to reduce the HPPH dihedral angle from 90° to *ca.* 45°, while the *trans*-like structure is obtained by rotating the same bonds so as to increase the dihedral angle to *ca.* 135°. The reason can be found in the peculiar properties of allenic structures. In the allene cation, removal of an electron from the truly degenerate π system results in a Jahn–Teller effect that induces rotation of the CH_2 groups by *ca.* 40°.[3] In the phosphorus compound, the unpaired electron resides in one of the π orbitals which were nearly degenerate in the neutral phosphallenic groups. The same kind of electronic effect that led to the geometry changes in allene operates here, leading to the rotation of the PH bond. But, due to the different local symmetry of the isovalent CH_2 and PH groups, clockwise and counterclockwise rotations no longer give the same geometry. In addition, we note that the PCP backbone remains practically linear (*ca.* 178°) in the *trans*-like structure while it bends to *ca.* 160° to accommodate the steric effect of the substituents in the *cis*-like one. Other modifications are only of marginal interest.

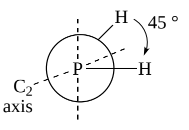

5

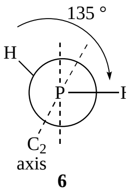

6

The stationary character of these points was assessed by vibrational analysis the results of which are reported in Table 3 for the most flexible basis set. In order to account for both the correlation still unbalanced at the MP2 level and the neglect of anharmonic effects, the computed frequencies have been scaled by 0.94 following the conclusions of previous studies on positive ions involving bonding between second and third row

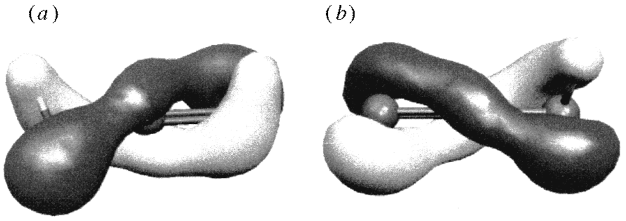

Fig. 2 Representation of the molecular orbital containing the unpaired electron in $\mathbf{2}^{\bullet+}$: (*a*) *cis*-like rotamer, (*b*) *trans*-like rotamer

atoms.[28] This value is consistent with that deduced from a recent systematic investigation of neutral systems.[29]

The main effect of ionization is to shift the stretching vibration of the allenic linkage towards lower frequencies, in agreement with the loss of an electron from a bonding system. The asymmetric vibrations that are strongly coupled are the more affected. It is the same vibrations that are at the origin of the short bond/long bond Jahn–Teller distortion already mentioned in allene.[3] The other vibrations (torsion, stretching and bending) are not significantly modified when going from the neutral system to the positive ions. The intensity of the asymmetric skeleton vibrations is greatly enhanced by ionization as already seen in positive ions generated by electron abstraction from a delocalized system.[30]

Hyperfine coupling constants were calculated for the *cis*- and *trans*-like structures optimized at the MP2 and MCSCF levels of wave functions. The corresponding values, obtained using the MP2 spin density after spin annihilation, are as follows:

$$\textit{cis}\text{-like}_{(\mathbf{MP2})}\ a(^{31}\mathrm{P}) = 140\ \mathrm{MHz};\ a(^{13}\mathrm{C}) = 76\ \mathrm{MHz}$$

$$\textit{trans}\text{-like}_{(\mathbf{MP2})}\ a(^{31}\mathrm{P}) = 141\ \mathrm{MHz};\ a(^{13}\mathrm{C}) = 84\ \mathrm{MHz}$$

$$\textit{cis}\text{-like}_{(\mathbf{MC})}\ a(^{31}\mathrm{P}) = 114\ \mathrm{MHz};\ a(^{13}\mathrm{C}) = 98\ \mathrm{MHz}$$

$$\textit{trans}\text{-like}_{\mathbf{MC}}\ a(^{31}\mathrm{P}) = 185\ \mathrm{MHz};\ a(^{13}\mathrm{C}) = 76\ \mathrm{MHz}$$

It can be seen that both structures give two ^{31}P isotropic coupling constants which are rather close to the ^{13}C coupling constant; moreover, this value is quite consistent with the experimental value (87 MHz).† The corresponding spatial distribution of the SOMO is illustrated in Fig. 2. The *ab initio* spin populations calculated for both rotamers ($\rho_{\mathrm{p(C)}}$ *ca.* 0.49; $\rho_{\mathrm{p(P)}}$ *ca.* 0.18) are in agreement with the values deduced from the estimation of the dipolar contributions presented in the preceding section.

Although all the calculation methods mentioned in Table 2 indicate that the optimized *cis*-like structure is slightly more stable than the *trans*-like structure, the corresponding energy difference is very small (Table 2) and implies that the two isomers are equally present in solution. In the present paragraph we will try to get some insight on the interconversion process between these two structures. The corresponding potential surface, has been mapped taking the HPPH dihedral angle as a distinguished coordinate,[31] *i.e.* a complete geometry optimization of the other structural parameters is performed for each selected angle. It showed a conical intersection for the perpendicular arrangement of the CPH planes which is accessible from both the *cis*(^{2}A$_2$) and *trans*(^{2}B$_g$) sides of the surface [Fig. 3(*a*)], even at the CASSCF level if only the lowest state is optimized. The dynamics of the coupling between the two parts of the surface is beyond the scope of this paper. Here, the conversion path between *cis*- and *trans*-like structures has been approximated by using the potential surface derived from the state-averaged CASSCF calculation involving the three lowest states that strongly interact along the rotation. Such a potential surface reproduces the stationary points and varies smoothly over the entire rotation [Fig. 3(*b*)] leading to a barrier of 9.04 kcal mol^{-1} above the *cis*-like minimum on the interconversion path.

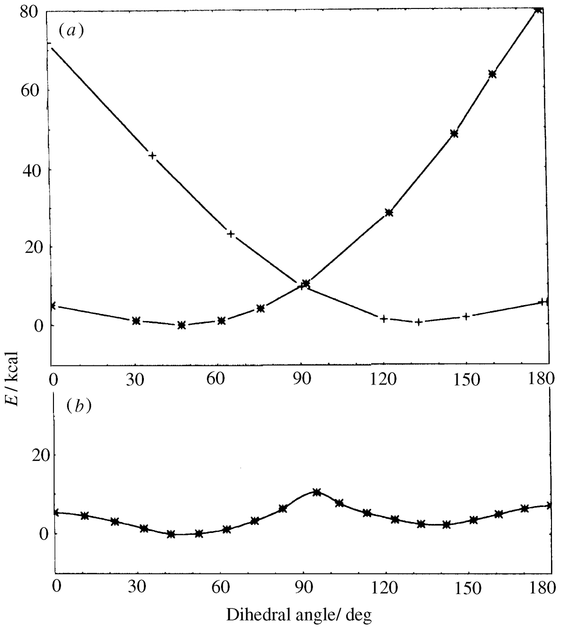

Fig. 3 Potential energy surface for $\mathbf{2}^{\bullet+}$ as a function of the HPPH dihedral angle: (*a*) CASSCF/6-31G** energy surface; (*b*) state-averaged CASSCF/6-31G** energy surface

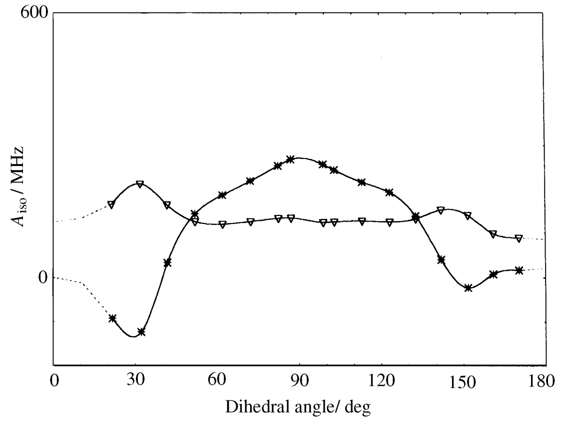

Fig. 4 Variation of the isotropic coupling constants of $\mathbf{2}^{\bullet+}$ with the HPPH dihedral angle (calculations at the MP2/6311G** level). ▽ represents the ^{13}C-A_{iso} values, * represents the ^{31}P-A_{iso} values.

For each value of the HPPH coordinate the corresponding coupling constants were evaluated at the MP2 level with spin annihilation. The coupling constants for (HPCPH)$^{\bullet+}$ in solution can then be calculated by averaging the coupling constant function [Fig. 1(*c*)] over the range of variation of HPPH. The averaged values‡ thus obtained are: $a(^{31}\mathrm{P}) = 98$ MHz and $a(^{13}\mathrm{C}) = 113$ MHz. Of course these values, calculated for (HPCPH)$^{\bullet+}$ are not totally relevant for the system $\mathbf{1}^{\bullet+}$ since we assumed a free rotation which may be hindered by the presence of the cumbersome Ar groups; nevertheless these calculated coupling constants remain quite compatible with the experimental constants obtained for $\mathbf{1}^{\bullet+}$. Moreover, this rotation process around the P···P axis may be related to the reversible appearance–disappearance of the signal observed when moni-

---

† The maximum difference between $a(^{13}\mathrm{C})$ and $a(^{31}\mathrm{P})$ occurs for the *trans*-like radical cation, this difference corresponds to a difference $\Delta\rho_{\mathrm{s}}$ equal to 0.006 between the carbon and phosphorus s-spin densities. This value is quite similar to that found when the two coupling constants are equal to 87 MHz ($\Delta\rho_{\mathrm{s}} = 0.017$).

‡ The three most contaminated values ($\langle S^2\rangle$ superior to 0.77) which correspond to the high energy conformations (HPPH = 0°, 10° and 180°) were discarded from the averaging procedure.

toring a cooling–heating protocol: when going from the liquid to the solid phase, rotation is impeded and the radical is frozen in random conformations, each one being characterized by different hyperfine tensors. Like the isotropic hyperfine constants (Fig. 4), the dipolar couplings τ are drastically dependant upon the HPPH dihedral angle (^{31}P-τ_{max} varies from 150 to 270 MHz and ^{13}C-τ_{max} varies between 31 and 41 MHz); the resulting broadening of the lines could explain the absence of a spectrum at low temperature.

Acknowledgements

This work was supported by a grant from the Swiss National Research Fund. The support of French CNRS–IDRIS is also greatly acknowledged.

References

1 R. J. Brudzinski and B. S. Hudson, *J. Am. Chem. Soc.*, 1990, **112**, 4963.
2 N. Koga and K. Morokuma, *J. Am. Chem. Soc.*, 1991, **113**, 1907.
3 E. Haselbach, *Chem. Phys. Lett.*, 1970, **7**, 428.
4 Y. Takemura and T. Shida, *J. Chem. Phys.*, 1980, **73**, 4133.
5 K. Haddaway, K. Somekawa, P. Fleming, J. A. Tossell and P. S. Mariano, *J. Org. Chem.*, 1987, **52**, 4239.
6 K. Lammertsma and P. v. R. Schleyer, *J. Am. Chem. Soc.*, 1990, **112**, 7935.
7 M. W. Wong and L. Radom, *J. Mol. Struct.*, 1989, **198**, 391.
8 R. Furet, R. L. Matcha and R. Fuchs, *J. Phys. Chem.*, 1986, **90**, 5571.
9 N. J. Fitzpatrick, D. F. Brougham, P. J. Goarke and M. T. Nguyen, *Chem. Ber.*, 1994, **127**, 969.
10 K. Toyota, M. Shibata and M. Yoshifuji, *Bull. Chem. Soc. Jpn.*, 1995, **68**, 2633.
11 *Multiple Bonds and Low Coordination in Phosphorus Chemistry*, eds. M. Regitz and O. Scherer, Thieme, New York, 1990.
12 (*a*) W. W. Schoeller, J. Niemann and R. Thiele, *Chem. Ber.*, 1991, **124**, 417; (*b*) M. Geoffroy, A. Jouaiti, G. Terron, M. Cattani-Lorente and Y. Ellinger, *J. Phys. Chem.*, 1992, **96**, 8241; (*c*) A. Jouaiti, M. Geoffroy, G. Terron and G. Bernardinelli, *J. Am. Chem. Soc.*, 1995, **117**, 2251; (*d*) W. W. Schoeller, W. Haug, J. Strutwolf and T. Busch, *J. Chem. Soc., Faraday Trans.*, 1996, **92**, 1751.
13 H. H. Karsh, H.-U. Reisacher and G. Müller, *Angew. Chem., Int. Ed. Engl.*, 1994, **23**, 618.
14 M. T. Nguyen and A. F. Hegarty, *J. Chem. Soc., Perkin Trans. 2*, 1985, 2005.
15 G. Frenking and H. Schwarz, *Z. Naturforsch., Teil B*, 1982, **37**, 1602.
16 M. W. Wong and C. Wentrup, *J. Am. Chem. Soc.*, 1993, **115**, 7743.
17 H. H. Karsch, F. H. Köhler and H.-U. Reisacher, *Tetrahedron Lett.*, 1984, **25**, 3687.
18 M. Yoshifuji, *J. Chem. Soc., Chem. Commun.*, 1984, 689.
19 L. Krieger, Ph.D. Dissertation, University of Bonn, Germany, 1988.
20 GAUSSIAN92, M. J. Frisch, G. W. Trucks, M. Head-Gordon, P. M. W. Gill, M. W. Wong, J. B. Foresman, B. G. Johnson, H. B. Schlegel, M. A. Robb, E. S. Replogle, R. Gomperts, J. L. Anders, K. Raghavachari, J. S. Binkley, C. Gonzalez, R. L. Martin, D. J. Fox, D. J. DeFrees, J. Baker, J. J. P. Stewart and J. A. Pople, Gaussian, Inc., Pittsburgh, PA, USA.
21 HONDO 8.5 from CHEM-Station, M. Dupuis, F. Jonhston and A. Marquez, 1994, IBM Corporation, Neighborhood Road, Kingston, NY 12401, USA.
22 P. Flukiger, *Development of Molecular Graphics Package MOLEKEL and its Applications to Selected Problems in Organic and Organometallic Chemistry*. Ph.D. Thesis No. 2561. University of Geneva, Switzerland, 1992.
23 J. R. Morton and K. F. Preston, *J. Magn. Reson.*, 1978, **30**, 577.
24 G. Ramakrishnan, A. Jouaiti, M. Geoffroy and G. Bernardinelli, *J. Phys. Chem.*, 1996, **100**, 10 861.
25 (*a*) T. Cole and C. Heller, *J. Chem. Phys.*, 1961, **34**, 1085; (*b*) H. M. McConnell, C. Heller, T. Cole and R. W. Fessenden, *J. Am. Chem. Soc.*, 1960, **82**, 766.
26 R. Bolze, H. Eierdanz, K. Schlüter, W. Massa, W. Grahn and A. Berndt, *Angew. Chem., Int. Ed. Engl.*, 1982, **21**, 924.
27 D. Feller, E. Huyser, W. T. Borden and E. R. Davidson, *J. Am. Chem. Soc.*, 1983, **105**, 1459.
28 (*a*) O. Parisel, M. Hanus and Y. Ellinger, *J. Phys. Chem.*, 1996, **100**, 2926; (*b*) O. Parisel, M. Hanus and Y. Ellinger, *J. Chem. Phys.*, 1996, **104**, 1979.
29 A. P. Scott and L. Radom, *J. Phys. Chem.*, 1996, **100**, 16 502.
30 (*a*) D. J. DeFrees, M. P. Miller, D. Talbi and Y. Ellinger, *Astrophys. J.*, 1993, **408**, 530; (*b*) S. R. Langhoff, *J. Phys. Chem.*, 1996, **100**, 2819.
31 (*a*) W. H. Miller, N. C. Handy and J. E. Adams, *J. Chem. Phys.*, 1985, **82**, 1281; (*b*) V. Barone, A. Grand, C. Minichino and R. Subra, in *Strategies and Applications in Quantum Chemistry*, eds. Y. Ellinger and M. Defranceschi, Kluwer, Dordrecht, 1996, p. 251.

Paper 6/07742K
Received 14*th November* 1996
Accepted 14*th January* 1997